Measurement of Supercritical CO_2 Plasticization of Poly(tetrafluoroethylene) Using a Linear Variable Differential Transformer

Ozge Guney-Altay, Suresh L. Shenoy,[†] Tomoko Fujiwara,[‡] Sadashige Irie,[§] and Kenneth J. Wynne*

Department of Chemical and Life Science Engineering, 601 W. Main Street, Virginia Commonwealth University, Richmond, Virginia 23284-3028

Received June 21, 2008; Revised Manuscript Received September 3, 2008

ABSTRACT: From measurements utilizing a linear variable differential transformer (LVDT), poly(tetrafluoroethylene) is found to undergo unusually high linear dilation in CO_2 at high temperatures and pressures. The extent of dilation and the dilational profiles are shown to depend strongly on molecular weight and crystallinity. It is also shown that the conditions at which melting and sintering occur can be identified from LVDT measurements. After the first heating cycle in CO_2, unsintered samples (PTFE-230, -600, -1000, and U-PTFE) show a T_m identical to PTFE (327 °C) instead of the higher pre-CO_2 T_m. This observation indicates that these samples were sintered during the LVDT measurements. ΔH_f was constant for pre-CO_2 PTFE-230, -600, and -1000, but after sintering, crystallinity decreased with increasing molecular weight. In contrast to the precipitous drop for U-PTFE, ΔH_f for PTFE-230, -600, and -1000 remained above 70 J/g. Chain entanglement effects on crystallization are modest for these low molecular weight materials. For lower molecular weight samples (PTFE-230, -600, and -1000), T_m depression and melt flow were observed. For the high molecular weight samples (PTFE and U-PTFE), T_m depression in CO_2 also occurs, but exceptionally high molecular weight and chain entanglement preclude melt flow. Both PTFE and U-PTFE are unusual in that melting is signaled by an increase in dilation rather than the usual loss of shape or "slumping" due to melt flow. Despite the hydrostatic pressure effect, PTFE melting point depression in supercritical CO_2 was found to be approximately 30 °C.

Introduction

Polytetrafluoroethylene (PTFE) exhibits a range of unique properties including chemical stability, lubricity, and a wide service temperature range (melting temperature, $T_m = 327$ °C).[1,2] Very high molecular weights (10^7-10^8 g/mol) are employed to inhibit crystallinity and provide chain entanglement for improved mechanical properties.[2,3]

As a result of extremely high molecular weight, PTFE has a high melt viscosity that precludes conventional melt processing.[1,2] While PTFE can be "processed" on a laboratory scale by shearing at 130 °C to yield highly oriented thin films[4] or by extrusion with an Instron capillary rheometer at 350 °C,[5] PTFE is processed commercially by sintering, ram extrusion, paste extrusion, and compression molding.[1,6,7] In an interesting advance, Tervoort and Smith found that addition of low molecular weight PTFE (up to 2.5×10^5 g/mol) decreased the melt viscosity and enabled conventional melt processing.[8,9] Compositional adjustment resulted in tensile bars and fibers with excellent mechanical properties.

Synthesis of PTFE in condensed CO_2 provides a novel alternative to conventional methods.[10] While PTFE is insoluble in CO_2, CO_2 plasticization has been shown to facilitate perfluoropolymer processing by reducing processing temperatures.[11–15] Venkataraman et al. was the first to demonstrate the use of high pressure CO_2 to generate PTFE foams.[16] Modification of a small extruder for use with high pressure CO_2 permitted the processing of intractable polymers including PTFE.[17] A continuous process was developed for generating foamed PTFE in CO_2 at 360 °C and 3.44 MPa. Under these conditions, CO_2 plasticization was responsible for the lower processing temperatures.[17] CO_2 plasticization was also used by Rajagopalan and McCarthy to facilitate the preparation of fluoropolymer−polymer composites.[18,19]

The studies noted above give evidence for the "CO_2-philic" nature of PTFE, but a systematic investigation of CO_2 solubility in PTFE has not been reported. Little swelling was observed at low pressures and temperatures in CO_2 (0.2% dilation at 42 °C and 22 MPa).[20] At moderate pressures (44 MPa) and slightly higher temperatures (80 °C) swelling increased to 5.5 vol %.[19]

Previously, we described a linear variable differential transformer (LVDT) system for the direct measurement of polymer swelling in high-pressure gases.[21] This method was subsequently used to investigate supercritical CO_2 plasticization of poly(vinylidene fluoride) (PVDF) and a PVDF copolymer.[11,22] In continuing the study of CO_2 interactions with fluorinated polymers we have investigated PTFE linear dilation in high pressure CO_2.[23] Preliminary LVDT results provided the basis for a report on improved PTFE mechanical properties by means of supercritical CO_2 processing.[24]

To probe more deeply the interaction of supercritical CO_2 and PTFE, a study of dilation versus pressure has been carried out. We report that very high linear dilation is found for PTFE in supercritical CO_2. For all temperatures tested, PTFE dilation was found to increase linearly with pressure. For one set of conditions, LVDT results are confirmed using a view cell. Complementary studies on the lower molecular weight PTFE samples and unsintered PTFE are discussed. Modulated differential scanning calorimetry (MDSC) and thermal expansion measurements are conducted to better understand and interpret the behavior of PTFE in supercritical CO_2.

* Corresponding author. Fax: (804) 828 3846; e-mail: kjwynne@vcu.edu.
[†] Current address: Philip Morris Research Laboratories, Richmond VA.
[‡] Current address: Department of Chemistry, University of Memphis, Memphis, TN 38152-3550.
[§] Current address: Daikin Industries, Ltd., 1-1 Nishi Hitotsuya, Settsu-Shi, Osaka 566-8585, Japan.

10.1021/ma8013977 CCC: $40.75
Published on Web 10/23/2008

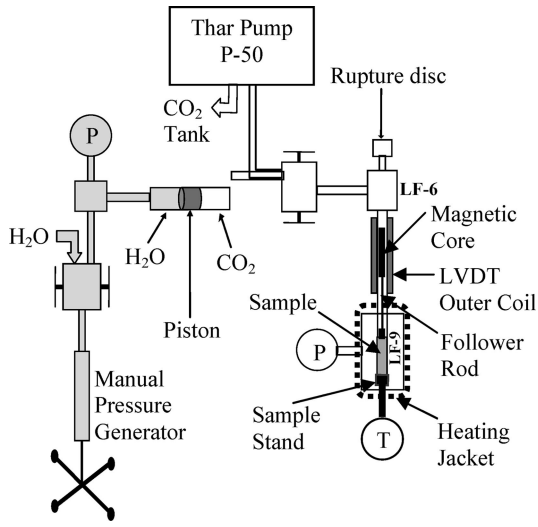

Figure 1. Schematic diagram of the LVDT setup used to measure linear dilation.

Experimental Section

Materials. For most polymers, a molecular weight of 230 000 g/mol would be considered "high molecular weight". This is not the case for PTFE. Lower molecular weight PTFE samples were provided by Daikin Industries, Ltd., Japan. These have designations PTFE-230, PTFE-600, and PTFE-1000, where the suffix is molecular weight in kg/mol. Unsintered PTFE is "as polymerized" M-18 designated U-PTFE (10^4-10^5 kg/mol; T_m = 345 °C) was provided by Daikin Institute of Advanced Chemistry and Technology, Orangeburg NY, in the form discs (50 mm diameter, 3−4 mm thickness). By "as polymerized" it is meant that the polymer is taken directly from the reactor (aqueous suspension polymerization) without any thermal processing. The conventional PTFE designation (no suffix) is used for Daikin M-18 (10^4-10^5 kg/mol; T_m = 327 °C) that was used for manufactured plaques. Lower molecular weight samples were compressed so as to obtain plaques but were not heated. For the LVDT experiments, rectangular bars (5 mm × 3.5 mm × 4 mm) were cut with a sharp razor. Liquid CO_2 (99.8%) was obtained from Roberts Gas Company.

Linear Expansion Equipment. The LVDT apparatus including the calibration procedure is similar to that described previously,[11,21] but several modifications were employed (Figure 1). One is the use of a programmable high pressure pump (Thar Industries, P-50) in conjunction with the manual pump (High Pressure Equipment, Erie, PA). The Thar pump allows rapid CO_2 pressure increase while the manual pump permits controlled lowering of CO_2 pressure. Another difference is the use of a modified LF-9 adaptor as the sample chamber. The center of this three-opening adaptor is connected to the steel pipe which contains the LVDT rod (Figure 1). The remaining ports on the LF-9 adaptor are used to monitor the temperature (resistive temperature device, RTD) and the pressure (Omega PX-602 with an accuracy of ±3 bar) of the sample chamber. The sample is placed at the center of the LF-9 adaptor, and a custom built heating jacket (BH Thermal Corp., Cleveland, OH) is used for efficient heating. Since high temperatures are employed for the dilation experiments, joints in and near the sample chamber are lubricated with an antiseize compound (Loctite Silver grade obtained from McMaster-Carr).

LVDT Measurement. Linear swelling was measured at both constant temperature and constant pressure. When LVDT readings remained constant for 30 min it was assumed that the sample attained dimensional equilibrium.

Constant Temperature (15−67 MPa). For each measurement, the sample is first heated to the desired temperature. CO_2 pressure is then increased to the desired value with the Thar pump. LVDT readings are noted at regular intervals. The manual generator is employed for lowering the pressure from 67 to 14 MPa in a stepwise manner, and LVDT readings are again noted at regular intervals.

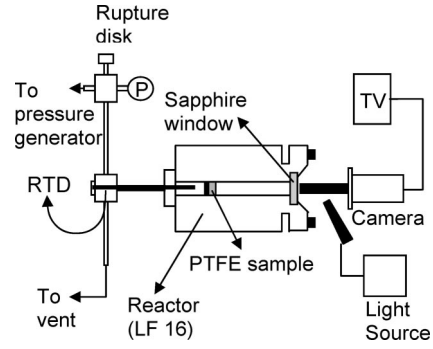

Figure 2. Schematic representation of the high-pressure view cell.

The LVDT data is recorded as voltage readings. To convert this data to the displacement of the follower rod, a calibration curve is obtained by placing the nonmagnetic follower rod on the central shaft of an accurate dial micrometer. Changes in LVDT readings are noted as the micrometer shaft was moved in small increments.

Constant Pressure. Previously we demonstrated that constant pressure measurements allow the observation of T_m depression as a function of CO_2 pressure.[11,22] In these experiments, CO_2 pressure is increased to a desired value and maintained at that value with the high pressure pump as the temperature is increased. When the swelling attained a steady value, the temperature is increased to the next value and the LVDT readings are noted.

View Cell. Figure 2 shows the schematic of the high-pressure view cell employed to observe PTFE swelling. The entire view cell assembly is made of 316-SS. The main body of the view cell consists of standard LF-16 tubing obtained from High Pressure Equipment (Erie, PA). One end of the LF-16 tubing is connected to a manual pressure generator (High Pressure Equipment, 37-6-30). The LF-16 cap seals the other end of the view cell. A sapphire disk supported by O-rings (Kalrez, Parker O-rings) in the LF-16 cap allows the observation of the PTFE sample in the chamber. The view cell is heated by a heating tape and is covered with insulation to minimize heat loss. The temperature and the pressure in the vessel are monitored via an RTD and a pressure transducer, respectively. Except for the sapphire window, the view cell consists of standard parts readily assembled with a torque wrench to manufacturer's specifications. PTFE swelling is recorded on a TV/VCR using a camera and a boroscope (Olympus Industrial).

Modulated Differential Scanning Calorimetry (MDSC). Temperature-modulated DSC was carried out using a TA-Q 1000 Series instrument (TA Instruments) with modulation amplitude of ±0.5 °C, modulation period of 30 s, and heating rate of 10 °C/min. Indium metal was used for calibration. The maximum melting endotherm is reported as the melting point (T_m). MDSC resolves the normal heat flow into reversing and nonreversing components[25,26] and thereby enables separation of transitions occurring in close proximity. Reversing heat flow curves are shown in Figures 3 and 9.

Safety. Working at high temperature and pressure requires equipment and procedural safety features. A rupture disk (85 MPa) was incorporated into the apparatus (Figure 1) and pressure was monitored in the sample chamber, at the high pressure pump, and at the manual pump. A 1/4 in. thick polycarbonate shield was secured between personnel and the high-pressure system.

Results and Discussion

All measurements start at 25 °C, just above the jump in expansion at 20 °C that corresponds to a MDSC endotherm ascribed to a PTFE crystal−crystal transition.[5] In each of the three sections below, ambient pressure MDSC and LVDT data are discussed followed by examination of linear expansion in supercritical CO_2. The first section focuses on lower molecular weight PTFE samples. Next, U-PTFE is discussed as it has a morphological connection to lower molecular weight materials and has a synthesis and processing link to PTFE. With this

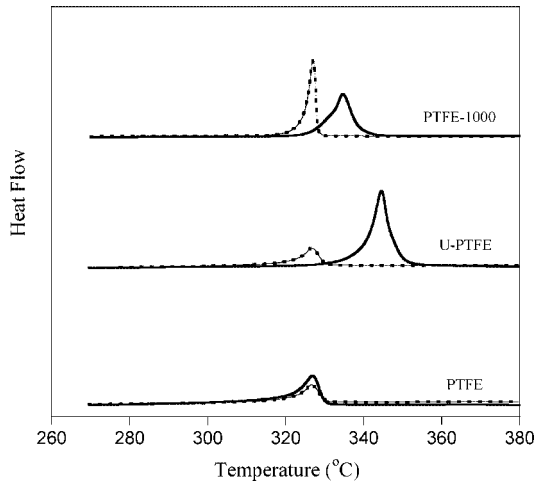

Figure 3. MDSC thermograms for PTFE-1000, U-PTFE, and PTFE. First heating (solid line); second heating (dashed line).

Table 1. Melting Points (T_m) and Heats of Fusion (ΔH_f) from MDSC

	first heating		second heating	
designation	T_m(°C)	ΔH_f (J/g)	T_m(°C)	ΔH_f (J/g)
PTFE-230	332	81	327	78
PTFE-600	334	89	327	75
PTFE-1000	335	85	327	71
U-PTFE	345	83	327	34
PTFE	327	34	327	41

background, the final section explores PTFE linear expansion at ambient pressure and in supercritical CO_2. These data add weight to Scheirs' statement that PTFE has the highest coefficient of thermal expansion for fluoropolymers (100×10^{-6} K^{-1}).[2]

1. PTFE-230, PTFE-600, and PTFE-1000. *Modulated Differential Scanning Calorimetry.* The thermograms for PTFE-230, PTFE-600, and PTFE-1000 are shown in Figure 1S, Supporting Information. The first and second heatings provide similar thermograms for all three materials. A representative thermogram for PTFE-1000 is shown in Figure 3. Melting points (T_m) and heats of fusion (ΔiH_f) are summarized in Table 1.

Examination of the data reported by Suwa shows a trend for increased T_m with molecular weight.[27] Table 1 confirms this trend T_m (332 − 335 °C) with increasing molecular weight (230−1000 kg/mol). The melting points of these three lower molecular weight PTFEs are 5−8 °C higher than PTFE but 10−13 °C lower than U-PTFE. The observation is consistent with increasing crystal perfection in the lower MW samples.

The enthalpies of melting for the lower molecular weight PTFEs are high (ΔH_f = 81−89 J/g) and similar to U-PTFE indicating high crystallinity. This result also suggests that ΔH_f is independent of molecular weight for all unsintered PTFE (see Table 1). A second scan of the lower molecular weight PTFEs gave melting points (327 °C) similar to PTFE. However, melting enthalpies (71−78 J/g) were still closer to U-PTFE (83 J/g) than PTFE (34−41 J/g). The difference in ΔH_f and consequently the crystallinity between the lower molecular weight PTFEs and PTFE confirm that for sintered PTFE, melting enthalpy decreases with increasing molecular weight.

Linear Dilation at Ambient Pressure. The percent linear dilation ($\Delta L_T/L_o$)% data for PTFE-1000 as a function of temperature at ambient pressure (thermal expansion) is shown in Figure 4, where ΔL_T is the change in sample length at a given temperature and L_o is the original sample length at ambient conditions. PTFE-230, PTFE-600, and PTFE-1000 have similar first-heating MDSC thermograms and T_ms, and their LVDT

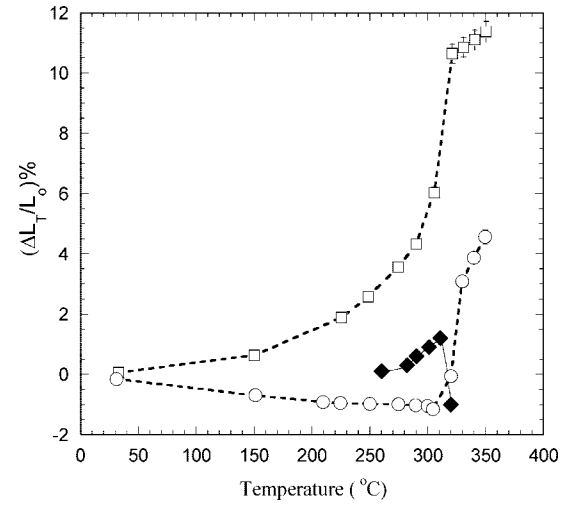

Figure 4. Linear dilation at ambient pressure (thermal expansion) measured by the LVDT technique: PTFE (□), U-PTFE (○), and PTFE-1000 (◆).

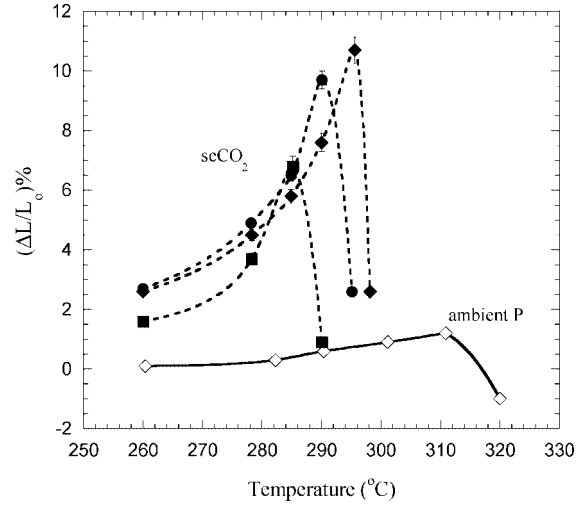

Figure 5. Linear dilation at constant pressure measured by the LVDT technique. At 67 MPa in CO_2: PTFE-230 (■), PTFE-600 (●), PTFE-1000 (◆). Ambient pressure data for PTFE-1000 (◇).

profiles are expected to follow the same trend as PTFE-1000 but were not investigated.

PTFE-1000 does not exhibit significant dilation below 250 °C (<0.1%). Between 250−300 °C increased dilation occurs, culminating with a maximum linear expansion of 1.2% at 311 °C followed by a marked decrease in linear expansion at 315 °C that indicates a loss of shape due to commencement of melting.[11,22] Interestingly, the linear expansion of PTFE-1000 is related to U-PTFE in that it is a highly crystalline material and has little expansion below 250 °C. However, a major difference is the observation conventional melting with flow for PTFE-1000 at 315 °C.

Linear Dilation in High Pressure CO_2. The effect of temperature on dilation of PTFE-230, PTFE-600, and PTFE-1000 at 67 MPa is shown in Figure 5. The percent dilation of PTFE-1000 as a function of temperature at ambient pressure is included for comparison. At ambient pressure, percent dilation for PTFE-1000 decreases at $T \geq 315$ °C, which is an indication of melt flow. At 67 MPa in CO_2, rapid softening is indicated by a decrease in percent dilation at 297 °C for PTFE-1000. In high pressure CO_2, the lowering of PTFE-1000 T_m (Δ = 18 °C) is due to CO_2 plasticization, which also results in an enhanced melt flow after melting.

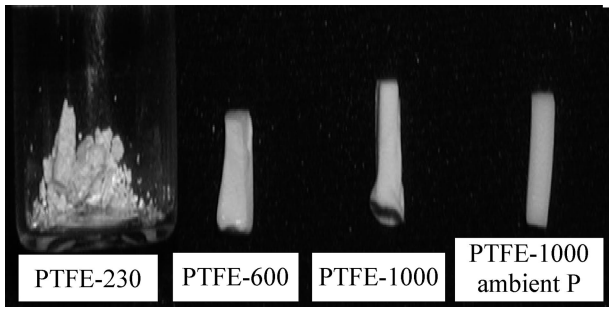

Figure 6. Images of lower molecular weight PTFE samples after the LVDT experiments described in Figure 5. All samples were rectangular bars prior to the LVDT constant pressure experiments.

For the series PTFE-230, PTFE-600, and PTFE-1000 at 67 MPa T_m is lowered to 287 °C, 293 °C, and 297 °C, respectively. The results suggest that chain end effects play a role in determining PTFE T_m in CO_2. Chain ends generally act as defects in the crystal structure.[28] In the presence of high pressure CO_2, chain ends are prone to melt early. As MW decreases, the number of chain ends increase and hence a greater degree of T_m depression is observed. CO_2 plasticization is also responsible for the greater extent in dilation observed for the lower molecular weight PTFEs compared to the ambient pressure data.

Figure 6 shows images of the post-CO_2 treated lower molecular weight PTFE samples (constant pressure experiments). All samples were rectangular bars prior to the LVDT constant pressure experiments and were kept in the sample chamber for 24 h after depressurization to ensure CO_2 elimination from the samples. The PTFE-230 sample has clearly lost shape integrity. On the other hand, PTFE-600 and PTFE-1000 show evidence of deformation indicating melt flow. In absence of CO_2 plasticization, the deformation of PTFE-1000 is significantly reduced. This is further evidence that high pressure CO_2 plasticizes PTFE, thereby decreasing melt viscosity and increasing deformability.

Percent dilation as a function of CO_2 pressure at 278 °C for PTFE-230, PTFE-600, and PTFE-1000 is shown in Figure 7a. Initially (<15 MPa) positive dilation is observed, but for pressures between 15 −30 MPa, a $(\Delta L/L_o)\%$ decreases, indicating that compression due to increased pressure dominates thermodynamic interactions. For pressures ≥41 MPa, $(\Delta L/L_o)\%$ increases for all samples to a maximum of 1.5%/55 MPa (PTFE-230), 2.7%/61 MPa (PTFE 600), and 4.5%/67 MPa (PTFE-1000).

At lower pressures (<30 MPa), dilational behavior reflects a competition between CO_2 plasticization and compression effects. At higher pressures, the order of maximum plasticization before melting (noted above) is not explained by differences in crystallinity, as ΔH_f for pre-CO_2 exposed samples is independent of molecular weight. Rather, the order of increased swelling with increased molecular weight suggests that within the transition region marked with dashed lines in Figure 7a, the samples are sintered. In semicrystalline polymers, solubility of CO_2 occurs solely in amorphous regions.[22] As high crystallinity inhibits swelling, the extent of dilation increases as molecular weight increases. The results are consistent with MDSC data (Table 1) that indicate post-CO_2 samples have crystallinity that decreases with increasing molecular weight. That is, as molecular weight increases, the amorphous domain produced in situ by sintering increases resulting in higher swelling by CO_2.

The plateau regions or attenuations observed for PTFE-230, PTFE-600, and PTFE-1000 denote that the plasticization effect of CO_2 is counterbalanced by the hydrostatic effect. Since CO_2 can only be dissolved in the amorphous domain, the plateau region is reached at lower pressures as the molecular weight decreases.

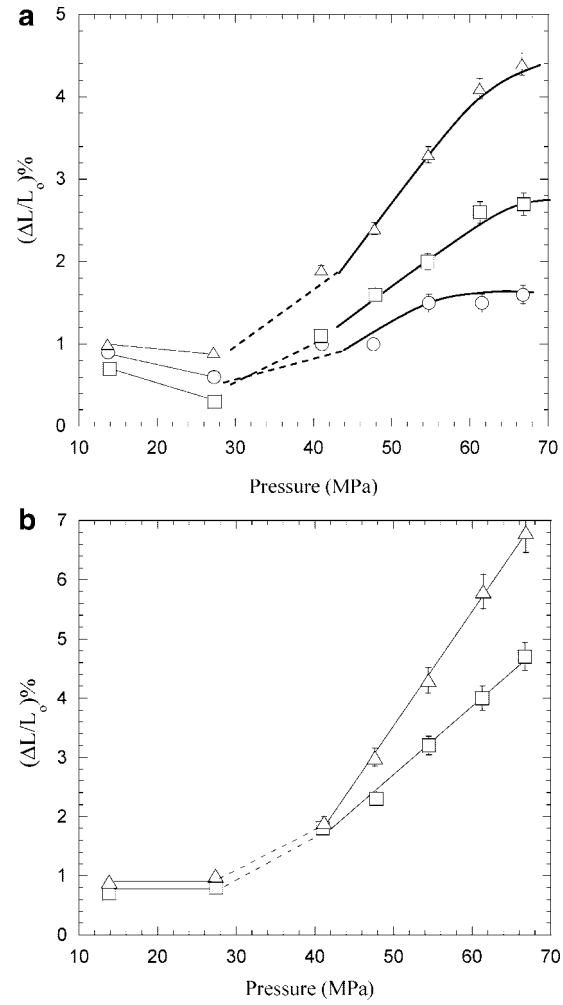

Figure 7. (a) Linear dilation of PTFE-230 (○), PTFE-600 (□), and PTFE-1000 (△) at 278 °C as a function of CO_2 pressure. (b) Linear dilation of PTFE-600 (□) and PTFE-1000 (△) at 290 °C as a function of CO_2 pressure.

Percent dilation as a function of CO_2 pressure at 290 °C for PTFE-600 and PTFE-1000 is shown in Figure 7b. A small (<1%) positive dilation is observed below 30 MPa. For pressures ≥41 MPa, $(\Delta L/L_o)\%$ increases linearly for both of samples, but the rate of change with pressure (i.e., the slope) is higher for PTFE-1000. At 67 MPa, $(\Delta L/L_o)\%$ are 4.7% and 6.8% for PTFE-600 and PTFE-1000, respectively. The percent linear dilation and post-CO_2 MDSC (Table 1) indicate that within the transition region marked with dashed lines in Figure 7b, PTFE-600 and PTFE-1000 are sintered.

At 67 MPa/290 °C, percent dilation observed are 4.7% and 6.8% for PTFE-600 and PTFE-1000, respectively. These values are greater than those observed at 278 °C (2.7% and 4.4% from Figure 7a). This is an interesting finding considering CO_2 density is 3% greater at 278 °C,[29] yet a 35−42% increase in dilation is observed at 290 °C. These results indicate that at 290 °C, there exists a greater fraction of amorphous content indicating commencement of melting. This observation is consistent with the T_m depression in high pressure CO_2.

2. U-PTFE. *Modulated Differential Scanning Calorimetry.* Figure 3 shows an MDSC thermogram (10 °C/min) for U-PTFE while values for T_m and ΔH_f are collected in Table 1. For U-PTFE both T_m (345 °C) and ΔH_f (83 J/g) are considerably higher than PTFE (T_m = 327 °C, ΔH_f = 34 J/g). The higher

value of ΔH_f for U-PTFE is an indication of higher crystallinity compared to PTFE, and the difference in T_m for PTFE and U-PTFE is attributed to morphological differences in agreement with prior work.[1,27,30–34] U-PTFE has an extended chain structure while PTFE has a folded chain structure.

The 345 °C T_m for U-PTFE is observed only for the first heating. All subsequent runs show a melting transition of 327 °C, indicating a folded chain structure. While U-PTFE undergoes sintering there is negligible particulate coalescence. Thus the morphology of as-polymerized U-PTFE is unique and is irreversibly changed on melting. For the second heating, a ΔH_f equal to that of PTFE is observed. This behavior is a consequence of the ultrahigh molecular weight of U-PTFE. Once U-PTFE is heated above T_m, on cooling the order required to restore its original crystallinity is not achieved because of chain entanglement.

Linear Dilation at Ambient Pressure. Figure 4 shows linear dilation of U-PTFE at ambient pressure $(\Delta L_T/L_o)\%$ as a function of temperature, where ΔL_T is the change in sample length at a given temperature and L_o is the original sample length at ambient conditions. For U-PTFE, negative dilation (to −1.2%) is observed up to 305 °C. In sample preparation, the high crystallinity and brittle nature of U-PTFE militates against compressive formation of a dense object. Negative thermal expansion may reflect incremental densification during heating or relaxation of orientation produced by compression molding. Above this temperature, thermal expansion increases rapidly to 3.1% at 330 °C and continues to increase linearly to 4.6% at 350 °C. Exceptionally high molecular weight and chain entanglement preclude flow for U-PTFE (T_m = 345 °C). Melting is signaled by an increase in dilation rather than the usual loss of shape due to melt flow; the latter is seen in the same figure for PTFE-1000.

The MDSC trace for U-PTFE (Figure 3) shows that melting commences at $T > 320$ °C while the corresponding temperature from LVDT technique is also 320 °C. This comparison of thermal (MDSC, Figure 3) and dilational data (Figure 4) demonstrates that the onset of dilational increase correlates well with commencement of melting.

Linear Dilation in High Pressure CO_2. Figures 8a and 8b show U-PTFE dilation, $(\Delta L/L_o)\%$, as a function of CO_2 pressure at 304 and 320 °C, respectively, where ΔL is the change in sample length at a given CO_2 pressure and temperature and L_o is the original sample length at ambient conditions. Figure 8a (filled symbols) shows that at the lower temperature (304 °C) there is negligible dilation up to 42 MPa. However, at 48 MPa, dilation increases rapidly to 30%. For CO_2 pressures greater than 48 MPa, dilation continues to increase linearly with a steep slope. The maximum $(\Delta L/L_o)\%$ observed is 70% at 67 MPa. This is higher than the dilation recorded for PTFE at the same conditions (55%, see Table 2).

Figure 8b (filled symbols) shows that at the higher temperature (320 °C), linear dilation is observed at as low as 15 MPa in contrast to the 304 °C data. Dilation increases from approximately 10% at 15 MPa to 17% at 27 MPa. On the other hand at 42 MPa, $(\Delta L/L_o)\%$ increases sharply to 40%. Finally, for pressures greater than 42 MPa, dilation increases linearly with CO_2 pressure. The maximum $(\Delta L/L_o)\%$ observed is 75% at 67 MPa. This is also higher than the dilation of PTFE at the same conditions (59%, see Table 2).

Analogous to the thermal expansion behavior, differences in the dilational behavior of U-PTFE and PTFE in CO_2 can be reconciled based on the morphological and crystal structure differences. U-PTFE has an extended chain structure while PTFE has a folded chain structure.[35] The degree of crystallinity for U-PTFE is approximately 92−98% while that of PTFE is only about 40%[36] and "rarely reaches 70%".[2] In the presence

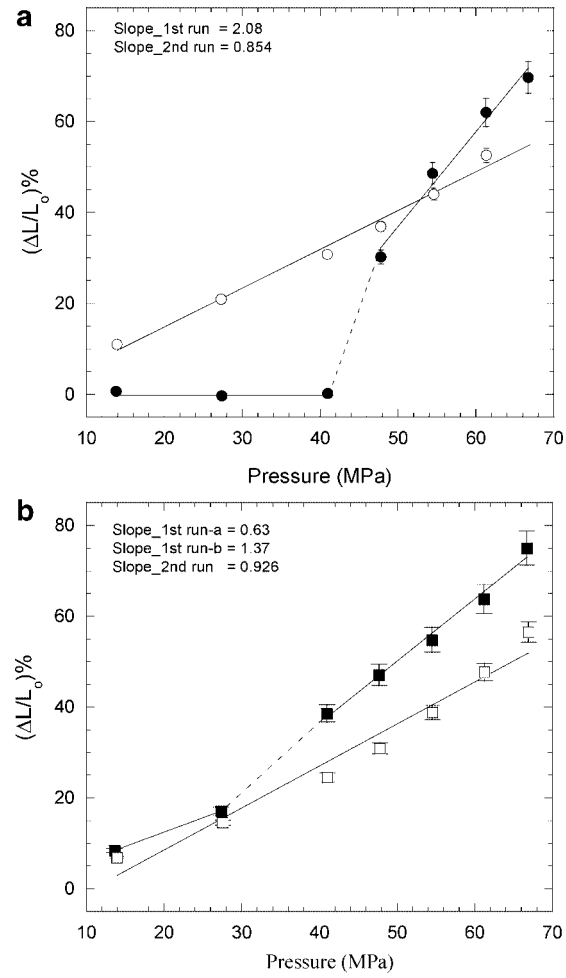

Figure 8. (a) Linear dilation of U-PTFE at 304 °C as a function of pressure. First run (●) and second run (○). (b) Linear dilation of U-PTFE at 320 °C as a function of pressure. First run (■) and second run (□).

of high pressure CO_2 at 304 °C, for pressures up to 42 MPa, the high degree of crystallinity inhibits U-PTFE dilation. On the other hand, large dilation observed for $P \geq 48$ MPa clearly indicates presence of amorphous content resulting from CO_2 plasticization. Thus at 304 °C and 42 MPa, the unsintered extended chain structure is changed to a folded chain structure increasing the amorphous content in the process. This is equivalent to the morphological change during the sintering process. At 320 °C and 15 MPa, dilation is 10%, indicating presence of amorphous fraction even at this low pressure. On the basis of our results, it can be concluded that the morphological changes may be occurring even at the lowest pressure, i.e. 15 MPa, at 320 °C. However, the sharp increase at 42 MPa suggests the extended chain crystal structure is completely destroyed for $P \geq 42$ MPa. At higher temperatures (>320 °C), lower pressures can be utilized to change U-PTFE morphology.

The results of second experimental runs using the same samples at identical conditions are also shown in Figures 8a and 8b. In the second runs (unfilled symbols), the dilational behavior observed is significantly different than that of the original U-PTFE samples. In both figures, a linear increase in dilation is observed at the constant slope of 0.89 ± 0.03. These linear profiles are similar to the ones observed for PTFE (Figure 11). This is further proof that the extended chain structure of U-PTFE is destroyed during the first run. In other words, it can be said that U-PTFE undergoes sintering. The maximum linear dilation observed in the second runs at 304 and 320 °C are 55% and 57%, respectively. These are lower than the values reported

Table 2. PTFE Linear Dilation Data Shown in Figures 10a and 10b

pressure (MPa)	temperature (°C)	original data ($\Delta L/L_o$)%	projected data ($\Delta L_T/L_o$)%	corrected data ($\Delta L_c/L_o$)%
67	260	11.3	3.8	7.5
	278	20.5	5.25	15.25
	290	46.8	9.4	37.4
	304	54.6	10.65	43.95
	320	58.9	11.3	47.6
62	260	10.5	4	6.5
	278	18.7	5.35	13.35
	290	41.9	9.7	32.2
	304	48.6	10.95	37.65
	320	51.6	11.5	40.1
56	260	9.6	4	5.6
	278	16.2	5.3	10.9
	290	34.3	9.2	25.1
	304	43.2	10.95	32.25
	320	45.5	11.5	34
48	260	8.4	3.9	4.5
	278	13.9	5.3	8.6
	290	31.6	9.4	22.2
	304	37.3	10.75	26.55
	320	38.8	11.1	27.7
42	260	7	3.9	3.1
	278	11.1	5	6.1
	290	21.3	7.6	13.7
	304	32.1	10.5	21.6
	320	33.4	10.85	22.55
29	260	4.9	3.85	1.05
	278	7.2	4.7	2.5
	290	11.5	6.3	5.2
	304	23.9	10.9	13
	320	24.6	11.2	13.4
15	260	2.8	4.2	−1.4
	278	3.7	4.95	−1.25
	290	5.5	6.5	−1
	304	9.2	9.7	−0.5
	320	10.6	10.85	−0.25
0.1	260	3.0	n/a	n/a
	278	3.7	n/a	n/a
	290	4.3	n/a	n/a
	304	5.8	n/a	n/a
	320	10.3	n/a	n/a

for the first run and closer to the values reported for PTFE (Table 2). We believe that the higher percent dilation observed in the first runs can be attributed to the additional expansion resulting from the irreversible crystal (0.2302 g/cm^3) to amorphous (2.06 g/cm^3) transition.[33,37]

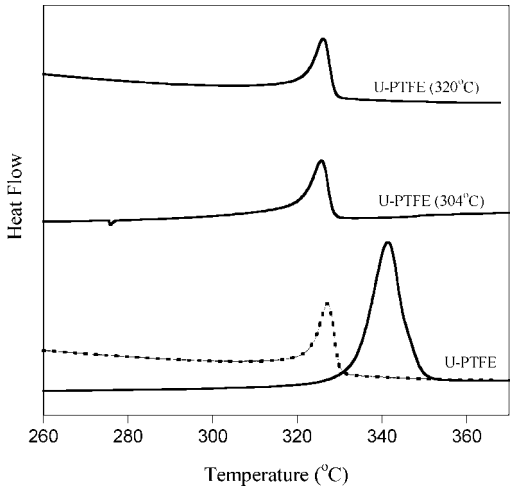

Figure 9. MDSC thermograms for U-PTFE samples after the linear dilation experiments at 304 and 320 °C for pressures to 67 MPa in CO_2. MDSC thermogram for U-PTFE is also included for comparison. First heating (solid line); second heating (dashed line).

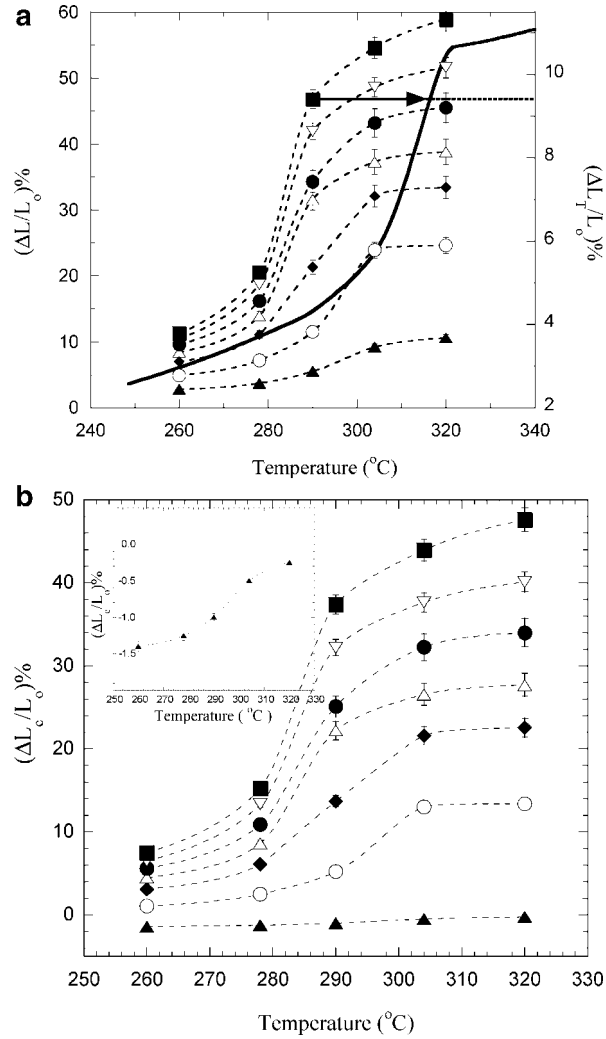

Figure 10. (a) PTFE linear dilation (dashed lines, left ordinate) as a function of temperature in CO_2 at various pressures in MPa; 15 (▲), 29 (○), 42 (◆), 48 (△), 56 (●), 62 (▽), and 67 (■). PTFE thermal expansion in N_2 at ambient pressure (solid line, right ordinate). (b) PTFE linear dilation corrected for thermal expansion and T_m depression as a function of temperature in CO_2 at various pressures in MPa; 15 (▲), 29 (○), 42 (◆), 48 (△), 56 (●), 62 (▽), and 67 (■).

Figure 9 shows the MDSC curves for the U-PTFE samples (both 304 and 320 °C) after the first runs. For comparison, both the first and the second MDSC scans of the as received U-PTFE are also included. It can be seen that the 345 °C melting peak is irreversible. The disappearance of the T_m = 345 °C is an indication of sintering. In addition, as expected, the crystallinity (as measured by area under the melting peak) is considerably lower in the second scans. Interestingly, both the 304 and 320 °C samples show only the 327 °C transition suggesting that exposure to high pressure CO_2 (15−67 MPa) has clearly altered U-PTFE morphology. Alternatively, it can be said that U-PTFE undergoes sintering during the LVDT experiments.

3. PTFE. *Differential Scanning Calorimetry.* Figure 3 shows the MDSC thermogram (10 °C/min) of PTFE while values for T_m and ΔH_f are collected in Table 1. For PTFE, a 327 °C melting endotherm and a ΔH_f of 34 J/g were observed. Both of these values are considerably lower than U-PTFE (T_m = 345 °C, ΔH_f = 83 J/g) and remain unchanged in consecutive heatings. As mentioned above, the higher value of ΔH_f for U-PTFE is an indication of higher crystallinity compared to PTFE, and the difference in T_m for PTFE and U-PTFE is attributed to morphological differences in agreement with prior work.[1,27,30–34]

Linear Dilation at Ambient Pressure. Linear dilation of PTFE at ambient pressure $(\Delta L_T/L_o)\%$ as a function of temperature is shown in Figure 4, where ΔL_T is the change in sample length at a given temperature and L_o is the original sample length at ambient conditions.

PTFE exhibited positive dilation at an increasing rate as a function of temperature for the full range of accessible temperatures. PTFE thermal expansion is 2.6% at 250 °C increasing to 5% at 300 °C. A remarkably rapid increase to 11% occurs between 300 and 350 °C for PTFE (T_m = 327 °C). Above T_m, the rate of increase in dilation attenuates. As for U-PTFE, melt flow is not observed for PTFE.

In conventional polymers such as PVDF, the LVDT technique provides an accurate determination of melting as sample-collapse results in a sharp decrease in the vertical dimension.[11,22] The absence of decrease in $(\Delta L_T/L_o)\%$ above T_m for PTFE and U-PTFE is due to exceptionally high molecular weight and chain entanglement that preclude flow. Both polymers are unusual in that melting is signaled by an increase in dilation rather than the usual loss of shape or "slumping" due to melt flow.

The MDSC trace for PTFE (Figure 3) shows that melting commences at $T > 310$ °C as indicated by an upturn in heat flow. This correlates with the accelerated increase in $(\Delta L_T/L_o)\%$ for $T > 300$ °C by the LVDT technique. The steadily increasing slope of the LVDT curve makes for low accuracy in the determination of the temperature for the onset of melting. This data provides further evidence that the onset of dilational increase correlates well with commencement of melting.

Analogous to ultrahigh molecular weight polyethylene, poly(tetrafluoroethylene) has several accessible solid-state structures.[38,39] U-PTFE has an extended chain structure[27,40,41] while the PTFE structure is a folded chain.[41–45] For PTFE, Khanna et al. proposed that the 327 °C transition represents a loss of folded chain order.[5] Recent simulations appear to confirm this hypothesis.[44,45] On the basis of the increasing rate of change in linear dilation, we propose that the helix to extended chain transition occurs over a broad temperature range rather than at the T_m. The higher dilation for PTFE is explained by the gradual uncoiling of PTFE folded chain conformation culminating at T_m. In contrast to 3.0% linear expansion for U-PTFE from 25−330 °C, we observed that PTFE thermal expansion in this range is 11%. The lower dilation of U-PTFE occurs because of the lower volume expansion in the transition from extended chain to melt compared to coil to melt for PTFE. While the contribution may be insignificant for small chains, the volume increase due to the unwinding of the helix will be amplified because of the high molecular weight of PTFE.

For PTFE, melting results in a lower order phase.[44,45] The higher temperature transition (~370 °C) observed by Khanna et al. corresponds to complete loss of order.[5] This temperature is above the range of the LVDT apparatus.

Linear Dilation in High Pressure CO_2. The temperature dependence of PTFE dilation in CO_2 was determined at seven different pressures (15, 29, 42, 48, 56, 62, and 67 MPa), and the data collected are depicted in Figure 10a. For polymers that exhibit negligible thermal expansion, dilation can be reported as percent change in sample length $(\Delta L/L_o)\%$, where ΔL is the change in sample length at a given CO_2 pressure and temperature and L_o is the original sample length at ambient conditions.[11,21,22] For PTFE, thermal expansion is substantial (Figure 4).

To obtain dilation due to CO_2 plasticization only, LVDT measurements were corrected for linear thermal expansion (ΔL_T). Linear dilation due to CO_2 sorption is reported as the change in sample length at a given CO_2 pressure and temperature with respect to L_{oT}, the original sample length corrected for thermal expansion ($L_{oT} = L_o + \Delta L_T$). However, this approach does not take the PTFE T_m depression observed in high pressure CO_2 into consideration. Thermal expansion observed at a temperature does not translate directly as the linear dilation contribution at that same temperature in high pressure CO_2. The sharp jump (between 300 and 327 °C) in linear dilation corresponding to PTFE melting at ambient pressure is shifted to lower temperatures in high pressure CO_2. The resemblance of the curves in Figure 10a to the PTFE thermal expansion profile in Figure 4 suggests that the underlying mechanisms resulting in dilation between 200 °C and complete melting in CO_2 and that for thermal expansion during melting at ambient pressure are similar.

PTFE linear dilation as a function of temperature at various pressures is characterized by S-shaped curves. As noted above, the culmination of the sharp increase in thermal expansion corresponds to complete melting at 0.1 MPa and 327 °C. Accordingly, it is proposed that the temperature at which rapid dilation ceases in high pressure CO_2 (304 °C) approximates the T_m of PTFE.

For all pressures tested, the important transitions that characterize the S-shaped curves (i.e., commencement, inflection point, and culmination) take place at the same temperatures. This must be due to the contravening effects of supercritical CO_2 plasticization and hydrostatic pressure. The increase in PTFE T_m with applied hydrostatic pressure is known (1.52 °C/MPa).[1] However, despite the hydrostatic pressure effect, PTFE melting point depression in supercritical CO_2 is about 30 °C.

To describe the procedure followed to incorporate empirically the PTFE T_m depression in high pressure CO_2 into the thermal expansion correction, the 67 MPa data in Figure 10a provides a representative example. The thermal expansion curve (Figure 4) was replotted on an expanded scale (right ordinate in Figure 10a) and brought in line with the 67 MPa data. The thermal expansion correction in high pressure CO_2 was then determined by a lateral shift indicated by the arrow in Figure 10a. The values are listed in Table 2 column labeled "projected $(\Delta L_T/L_o)\%$". The corrected data, $(\Delta L_c/L_o)\%$, is plotted in Figure 10b and tabulated in Table 2. ΔL_c is the change in sample length at a given CO_2 pressure and temperature with respect to the sample length corrected for thermal expansion and T_m depression.

The magnitude of swelling is quite striking, considering again the contravening effects of supercritical CO_2 plasticization and hydrostatic pressure. That is, the uncoiling of the helix is inhibited by the hydrostatic pressure, while mobility of the amorphous phase is increasing due to CO_2 plasticization. The data presented here suggest that thermodynamic interactions rather than hydrodynamic forces dominate the behavior of PTFE in supercritical CO_2. Even at 15 MPa (insert, Figure 10b), while the percent dilation is less than the thermal expansion at ambient conditions due to hydrostatic pressure as indicated by the negative values, the general trend of the data is still the same supporting the above argument.

Figure 11 illustrates the pressure dependence of the corrected percent dilation $(\Delta L_c/L_o)\%$ for different temperatures. The incremental increase in swelling for an increase in CO_2 pressure (i.e., the slope) is a strong function of temperature and increases with increasing temperature. $(\Delta L_c/L_o)\%$ increases linearly with pressure for the two lower (260, 278 °C) and higher (304, 320 °C) temperatures. The slope, $d(\Delta L_c/L_o)/dP$, at 260 °C is 0.17 MPa^{-1} and almost doubles to 0.32 MPa^{-1} at 278 °C. For the higher temperatures, the slope increases markedly to a constant value of 0.86 ± 0.03 MPa^{-1}. The increasing slopes at the lower temperatures are due to decreased physical cross-linking associated with continuous reduction in crystalline junction density as temperature approaches T_m. The constant slope, 0.86 ± 0.03 MPa^{-1}, indicates PTFE is melted. Interestingly, there is a break in the 290 °C isotherm. The slope for the lower pressures (≤30 MPa) is 0.37 MPa^{-1} but above 40 MPa the slope shifts to that

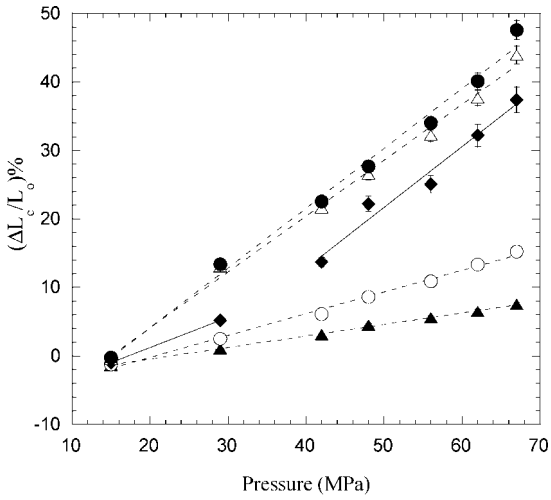

Figure 11. PTFE linear dilation as a function of CO_2 pressure at various temperatures in °C; 260 (▲); 278 (○); 290 (◆), 304 (△), and 320 (●). Note that the data has been corrected to eliminate the contribution due to thermal expansion and T_m depression.

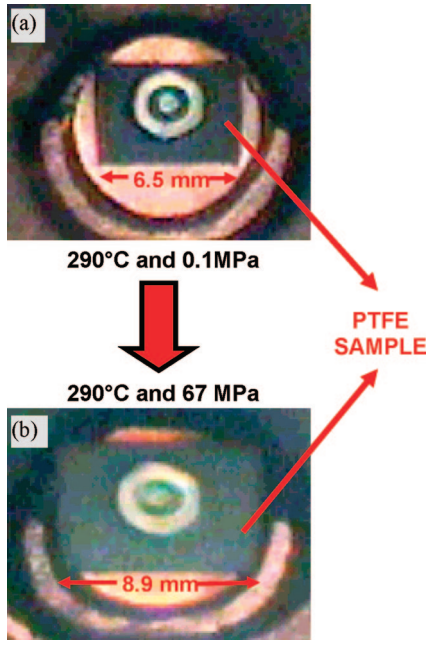

Figure 12. Verification of the unusually high PTFE dilation in supercritical CO_2 by view cell. (a) 290 °C, 0.1 MPa and (b) after 1 h at 290 °C, 67 MPa.

of the melt (0.86 ± 0.03 MPa^{-1}). The 290 °C isotherm in Figure 11 captures the melting transition with a change in slope at 40 MPa, which is consistent with the expected T_m depression discussed above.

The increase in the amount of amorphous fraction increases the solubility of CO_2 in PTFE. At very high pressures (≫67 MPa) it is possible that enhanced CO_2 solubility in the entangled melt will lower the entanglement density sufficiently to permit melt flow.[37,46]

Linear Dilation by High Pressure View Cell. To verify the unusually large PTFE dilation, we employed a view cell to track dilation visually. In Figure 12a, a PTFE sample is shown at 290 °C prior to CO_2 pressurization. The copper disk (8 mm diameter) in the background was used as a reference to estimate the change in the dimensions of the PTFE sample. Upon CO_2 pressurization to 67 MPa, the system was equilibrated for 1 h prior to recording PTFE dilation and image (Figure 12b). Figure 12b shows that the width of the PTFE sample has increased by ~40%, in agreement with LVDT measurements.

Conclusions

In contrast to lower molecular weight and less crystalline perfluorinated polymers,[47] PTFE is unaffected by a wide range of reagents and organic solvents. This is considered to be an advantage of PTFE in applications such as microstructural fabrication processes. However, from measurements utilizing a linear variable differential transformer (LVDT), poly(tetrafluoroethylene) is found to undergo unusually high swelling in CO_2 at high temperatures and pressures. The extent of dilation and the dilational profiles are shown to depend strongly on molecular weight and crystallinity. It is also shown that the conditions at which melting and sintering occur can be identified from LVDT measurements.

After the first heating cycle in CO_2 unsintered samples (PTFE-230, PTFE-600, PTFE-1000, and U-PTFE) show a T_m identical to PTFE (327 °C) instead of the higher pre-CO_2 T_m. In agreement with a previous report for U-PTFE,[16] this observation indicates that samples were sintered during the LVDT measurements. ΔH_f was constant for pre-CO_2 PTFE-230, -600, and -1000, but after sintering, crystallinity decreased with increasing molecular weight. In contrast to the precipitous drop for U-PTFE, ΔH_f for PTFE-230, -600, and -1000 remained above 70 J/g. Chain entanglement effects on crystallization are modest for these low molecular weight materials.

The dilational profiles for the lower molecular weight samples also confirmed these findings. The extent of dilation was highest for PTFE-1000 and decreased with decreasing molecular weight. At 278 °C and 67 MPa, percent dilation $(\Delta L/L_o)\%$ for PTFE-230, -600, and -1000 was 1.6, 2.7, and 4.4%, respectively, compared to 20.5% for PTFE (Figure 2S, Supporting Information). The rate of dilational change with pressure, i.e. the slope $d(\Delta L/L_o)/dP$, increases sharply from 0.093 for PTFE-1000 to 0.332 for PTFE. These results show that molecular weight has an important influence on maximum linear dilation and the rate of change of dilation with pressure.

For post-CO_2 U-PTFE, both T_m and ΔH_f were similar to PTFE, showing that the U-PTFE-extended chain morphology and high crystallinity are not recoverable after melt processing. The MDSC data in Table 1 show that as molecular weight decreases from 10 000 kg/mol to 1000 kg/mol, ΔH_f increases by 150% from 34 J/g to 85 J/g. These data are consistent with the findings of Wlochowicz et al. who found a critical MW of 4000 kg/mol.[3] Below this critical value, PTFE tensile strength and elongation decrease markedly. The brittle nature of low MW PTFE correlates with high crystallinity and low solubility of CO_2.

For the lower molecular weight samples (PTFE-230, -600, and -1000), T_m depression and melt flow were observed. For the high molecular weight samples (PTFE and U-PTFE), T_m depression in CO_2 also occurs, but exceptionally high molecular weight and chain entanglement preclude melt flow. Both PTFE and U-PTFE are unusual in that melting is signaled by an increase in dilation rather than the usual loss of shape or "slumping" due to melt flow. Despite the hydrostatic pressure effect, PTFE melting point depression in supercritical CO_2 was found to be approximately 30 °C.

T_m depression is an indication of the plasticization effect of CO_2 on PTFE. Our results constitute a thorough LVDT study tracing the $P-T$ plane that shows the PTFE melting transition in CO_2. The slope of percent dilation versus pressure is a strong function of temperature and increases with increasing temperature. The observed increase in slope with temperature is due to decreased physical cross-linking associated with continuous reduction in crystalline junction density as temperature ap-

proaches T_m. Accordingly, melting is indicated by the constant slope, 0.86 ± 0.03 MPa^{-1}, observed for $T > 290$ °C for PTFE. Interestingly, there is a break in the 290 °C isotherm. The slope for the lower pressures ($\leq$30 MPa) is 0.37 MPa^{-1}, but above 40 MPa the slope shifts to that of the melt. The 290 °C isotherm in Figure 11 captures the melting transition with a change in slope at 40 MPa, which is consistent with the expected T_m depression. The constant slope reported for the second runs in Figures 8a and 8b for U-PTFE at 304 and 320 °C is the same as PTFE, confirming our conclusion that during the first run, U-PTFE goes through sintering.

The marked T_m depression and high solubility of CO_2 in PTFE at elevated temperatures and pressures suggests CO_2-facilitated processing.[17] Guided by the results herein, we have recently found that conventional PTFE can indeed be injection molded in the presence of $scCO_2$. The results of this ongoing research will be the subject of a forthcoming paper.

Acknowledgment. K.J.W. thanks the Daikin Institute for Advanced Chemistry and Technology (DAI-ACT), NASA (Grant Numbers NAG5-12560 and NNC04GB13G), and the VCU School of Engineering Foundation for partial support of this research.

Supporting Information Available: Experimental details. Figure 1S, DSC thermograms for PTFE-230, PTFE-600, and PTFE-1000; Figure 2S, linear dilation at 278 °C as a function of CO_2 pressure for these same materials. This information is available free of charge via the Internet at http://pubs.acs.org.

References and Notes

(1) Gangal, S. V.; Grot, W. In *Encyclopedia of Polymer Science and Engineering*; John Wiley & Sons: New York, 1989; Vol. 16, pp 577−648.
(2) Scheirs, J. *Modern Fluoropolymers: High Performance Polymers for Diverse Applications*; John Wiley & Sons: New York, 1997.
(3) Wlochowicz, A.; Scigala, R. *Br. Polym. J.* **1989**, *21*, 205–207.
(4) Wittmann, J. C.; Smith, P. *Nature* **1991**, *352*, 414–417.
(5) Khanna, Y. P.; Chomyn, G.; Kumar, R.; Murthy, N. S.; O'Brien, K. P.; Reimschuessel, A. C. *Macromolecules* **1990**, *23*, 2488–2494.
(6) Ebnesajjad, S. *Fluoroplastics: The Definitive User's Guide and Databook*; Plastics Design Library: Norwich, NY, 2003; Vol. 2.
(7) Ochoa, I.; Hatzikiriakos, S. G.; Mitsoulis, E. *Int. Pol. Process.* **2006**, *21*, 497–503.
(8) Tervoort, T.; Visjager, J.; Graf, B.; Smith, P. *Macromolecules* **2000**, *33*, 6460–6465.
(9) Tervoort, T.; Visjager, J.; Smith, P. *J. Fluorine Chem.* **2002**, *114*, 133–137.
(10) Romack, T. J.; Kipp, B. E.; DeSimone, J. M. *Macromolecules* **1995**, *28*, 8432–8434.
(11) Shenoy, S. L.; Fujiwara, T.; Wynne, K. J. *Macromolecules* **2003**, *36*, 3380–3385.
(12) Wang, W. C. V.; Kramer, E. J.; Sachse, W. H. *J. Polym. Sci., Part B: Polym. Phys.* **1982**, *20*, 1371–1384.
(13) Wissinger, R. G.; Paulaitis, M. E. *J. Polym. Sci., Part B: Polym. Phys.* **1991**, *29*, 631–633.
(14) Zhang, Z. Y.; Handa, Y. P. *Macromolecules* **1997**, *30*, 8505–8507.
(15) Zhang, Z. Y.; Handa, Y. P. *J. Polym. Sci., Part B: Polym. Phys.* **1998**, *36*, 977–982.
(16) Venkataraman, S. K. US 5,912,278, **1999**.
(17) Garcia-Leiner, M.; Lesser, A. J. *J. Appl. Polym. Sci.* **2004**, *93*, 1501–1511.
(18) Arora, K. A.; Lesser, A. J.; McCarthy, T. J. *Macromolecules* **1999**, *32*, 2562–2568.
(19) Rajagopalan, P.; McCarthy, T. J. *Macromolecules* **1998**, *31*, 4791–4797.
(20) Briscoe, B. J.; Zakaria, S. *J. Polym. Sci., Part B: Polym. Phys.* **1991**, *29*, 989–999.
(21) Shenoy, S.; Woerdeman, D.; Sebra, R.; Garach-Domech, A.; Wynne, K. J. *Macromol. Rapid Commun.* **2002**, *23*, 1130–1133.
(22) Shenoy, S. L.; Fujiwara, T.; Wynne, K. J. *Macromol. Symp.* **2003**, *201*, 171–178.
(23) Ohsaka, Y.; Wynne, K.; Shenoy, S.; Irie, S. US 6,960,633, **2005**.
(24) Sun, H. L.; Cooke, R. S.; Bates, W. D.; Wynne, K. J. *Polymer* **2005**, *46*, 8872–8882.
(25) Boller, A.; Okazaki, I.; Wunderlich, B. *Thermochim. Acta* **1996**, *284*, 1–19.
(26) Verdonck, E.; Schaap, K.; Thomas, L. C. *Int. J. Pharm.* **1999**, *192*, 3–20.
(27) Suwa, T.; Seguchi, T.; Takehisa, M.; Machi, S. *J. Polym. Sci., Part B: Polym. Phys.* **1975**, *13*, 2183–2194.
(28) Flory, P. J. *Principles of Polymer Chemistry*; Cornell University Press: Ithaca, NY, 1953.
(29) Vargaftik, N. B. *Tables on the Thermophysical Properties of Liquids and Gases; 2nd Ed.*; John Wiley & Sons: New York, 1975.
(30) Grebowicz, J.; Pan, R.; Wunderlich, B. *J. Appl. Polym. Sci.* **1989**, *38*, 707–716.
(31) Jaffe, M.; Wunderlich, B. *Journal of Thermal Analysis and Calorimetry* **1969**, *1*, 387–403.
(32) Khanna, Y. P. *Journal of Materials Science Letters* **1988**, *7*, 817–818.
(33) Starkweather, H. W., Jr. *J. Polym. Sci., Part B: Polym. Phys.* **1982**, *20*, 2159–2161.
(34) Starkweather, H. W., Jr. *J. Polym. Sci., Part B: Polym. Phys.* **1985**, *23*, 1177–1185.
(35) Clark, E. S. *Polymer* **1999**, *40*, 4659–4665.
(36) Androsch, R.; Wunderlich, B.; Radusch, H. J. *J. Thermal Anal. Calorim.* **2005**, *79*, 615–622.
(37) Dee, G. T.; Sauer, B. B.; Haley, B. J. *Macromolecules* **1994**, *27*, 6106–6111.
(38) Zachariades, A. E.; Watts, M. P. C.; Porter, R. S. *Polym. Eng. Sci.* **1980**, *20*, 555–561.
(39) Zwijnenburg, A.; Van Hutten, P. F.; Pennings, A. J.; Chanzy, H. D. *Colloid Polym. Sci.* **1978**, *256*, 729–740.
(40) Melillo, L.; Wunderlich, B. *Kolloid Z. Z. Polym.* **1972**, *250*, 417–425.
(41) Wunderlich, B.; Moeller, M.; Grebowicz, J.; Baur, H. *Thermochim. Acta* **1988**, *135*, 8.
(42) Bunn, C. W.; Howells, E. R. *Nature* **1954**, *174*, 549–551.
(43) Kimmig, M.; Strobl, G.; Stuehn, B. *Macromolecules* **1994**, *27*, 2481–2495.
(44) Sprik, M.; Roethlisberger, U.; Klein, M. L. *J. Phys. Chem. B* **1997**, *101*, 2745–2749.
(45) Sprik, M.; Rothlisberger, U.; Klein, M. L. *Mol. Phys.* **1999**, *97*, 355–373.
(46) Tuminello, W. H.; Treat, T. A.; English, A. D. *Macromolecules* **1988**, *21*, 2606–2610.
(47) Lugert, E. C.; Lodge, T. P.; Buhlmann, P. *J. Polym. Sci., Part B: Polym. Phys.* **2008**, *46*, 516–525.

MA8013977